高频感应钎焊中电源频率的优化选择

何 鹏, 刘 多, 冯吉才
(哈尔滨工业大学 现代焊接技术国家重点实验室, 哈尔滨 150001)

摘 要: 在高频感应钎焊的过程中, 要获得良好的钎焊接头, 必须要根据接头材料的物理性能选择合适频率的高频电源, 采用计算机数值分析手段建立了感应加热电源及其频率范围的选择数值分析模型。研究表明, 数值解析法可以作为高频感应钎焊感应加热设备设计的重要方法。在对高频电源电流频率等参数的选择时, 利用数值解析模型所得到的解析近似解进行频率选择比传统经验公式更精确。因为后者由平面电磁波在导电媒质中的传播特性导出, 更适合于板状结构感应加热时频率的选择。而对于管状或其它复杂形状, 利用数值解析解可以较好地对高频电源的频率进行优化选择。

关键词: 高频感应钎焊; 电源频率; 数值解析; 优化选择
中图分类号: TG402 文献标识码: A 文章编号: 0253-360X(2005)11-27-03

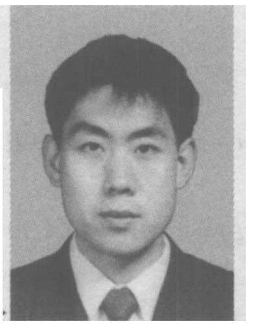

何 鹏

0 序 言

高频感应钎焊具有高效、控制精确、低污染等特点, 是一种环保型的钎焊方法[1,2]。要获得良好的钎焊接头, 必须根据接头材料的物理性能选择合适频率的高频电源, 而传统的基于试验及经验的频率选择方法往往费时费力, 随意性大, 亟待探寻新的方法对高频电的频率进行优化选择。使用计算机辅助设计可以节省时间, 减轻劳动强度, 提高生产率。作者采用物理数学解析手段建立起感应加热电源及其频率范围的数值选择模型, 并经试验验证, 获得了较好的效果[1,2]。

1 高频涡流问题的解析近似解

对于图 1所示管道的感应加热问题, 若假设线圈电流沿轴向均匀分布, 则可简化为一维模型。以此简化模型为对象, 使用解析法求出管道温度分布的积分公式, 这对于感应加热电流频率的选择具有一定的指导意义。

1.1 磁场的贝塞尔函数解

由矢量运算公式 $\nabla\times\nabla\times H=\nabla(\nabla\cdot H)-\nabla^2 H$ 可得柱坐标系中

$$r^2\frac{\partial^2 H_{2z}}{\partial r^2}+r\frac{\partial H_{2z}}{\partial r}+k^2r^2H_{2z}=0, \qquad (1)$$

收稿日期: 2005-09-15
基金项目: 国家自然科学基金资助项目(50505008)

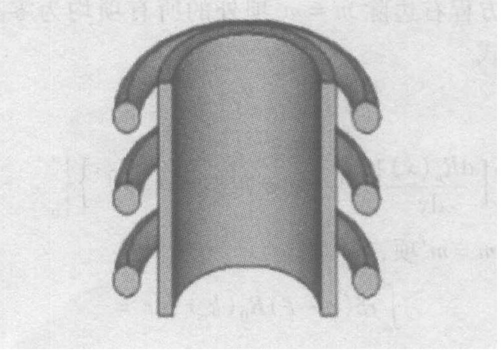

图 1 管道的感应加热

Fig. 1 Induction heating for pipe structure

式中: $k=\omega\sqrt{\mu\sigma}$。

分界面 $r=a$ 处的衔接条件为 $-\frac{1}{\sigma}\frac{\partial H_{1z}}{\partial r}\Big|_{r=a}=-\frac{1}{j\omega\varepsilon}\frac{\partial H_{2z}}{\partial r}\Big|_{r=a}$, $H_{1z}|_{r=a}=H_{2z}|_{r=a}$; 边界 $r=b$ 处满足, $H_{1z}|_{r=b}=\frac{NI}{L}$, 边界 $r=0$ 处满足 $\frac{\partial H_{2z}}{\partial r}\Big|_{r=0}=0$, 由式(1)即可求感应加热问题的电磁场的解析解。

1.2 温度场的格林函数解

格林函数又称为点源影响函数, 它表示一个点源在一定的边界条件和初值条件下所产生的场或影响。格林函数法的基本思想是首先考虑集中于一点的干扰, 然后根据问题的线性特点, 将对应于各个点源的解叠加起来, 即可求出定解问题的解。

1.2.1 有界区域热传导问题的格林函数

在柱坐标系中, 图 1所示感应加热问题的温度

场控制方程和边界条件[5,6]可表示为

$$\frac{\partial u}{\partial t}-a^2\Delta^2 u=f(r,t), \quad (2)$$

式中：$a^2=\lambda/\rho c$，$f(r,t)=J_m^2(r,t)/2\sigma\rho c$；$\lambda$ 为热导率；ρ为密度；c为比热。与之相应的格林函数为

$$\frac{\partial G}{\partial t}-a^2\Delta^2 G=\delta(r-\xi,t-\tau), \quad (3)$$

$$G|_{t=0}=0, \quad (4)$$

$$\left.\frac{\partial G}{\partial r}\right|_{r=a}=0,\ \left.\frac{\partial G}{\partial r}\right|_{r=b}=0. \quad (5)$$

利用 $r=a$处，$r=b$处的边界条件得

$$\delta(r-\xi)=\sum_{m=1}^{\infty}A_m\left[J_0(k_m r)-\frac{J_1(k_m b)}{N_1(k_m b)}N_0(k_m r)\right]。\quad (6)$$

式(6)的系数可由正交归一化条件确定。在该式两边乘以 $rR_0(k_m r)$，并从 $a\sim b$积分，由公式

$$\int_a^b rR_n(k_m r)R_n(k_m r)\,\mathrm{d}r=0。\quad (7)$$

可知方程右边除 $m=m$ 项外的所有项均为零。利用公式

$$\int_0^a x[R_n(x)]^2\mathrm{d}x=$$

$$\frac{1}{2}\left\{x^2\left[\frac{\mathrm{d}R_n(x)}{\mathrm{d}x}\right]^2+(x^2-n^2)[R_n(x)]^2\right\}\Big|_0^a。\quad (8)$$

可得 $m=m$ 项，有

$$\int_a^b r\delta(r-\xi)R_0(k_m r)\,\mathrm{d}r=$$

$$\frac{A_m}{2}\left\{b^2[R_0(b)]^2-a^2[R_0(a)]^2\right\}, \quad (9)$$

系数
$$A_m=\frac{2\int_a^b r\delta(r-\xi)R_0(k_m r)\,\mathrm{d}r}{\left\{b^2[R_0(b)]^2-a^2[R_0(a)]^2\right\}}。$$

1.2.2 温度场的积分公式

若在 $G(r,\xi,t,\tau)$中视(x,t)为参变量，(ξ,τ)为自变量，则 G满足[7,8]

$$-\frac{\partial G}{\partial\tau}-a^2\Delta^2 G=\delta(r-\xi,t-\tau), \quad (10)$$

$$\left.\frac{\partial G}{\partial\xi}\right|_{\xi=a}=0,\ \left.\frac{\partial G}{\partial\xi}\right|_{\xi=b}=0. \quad (11)$$

应用格林公式，并对时间导数部分积分得

$$I=-\int_{\partial\Omega}G(r,\xi,t,\tau)u(\xi,\tau)\mathrm{d}\xi+a^2\iint_{\partial\Omega}\left(u\frac{\partial G}{\partial\xi}-G\frac{\partial u}{\partial\xi}\right)\mathrm{d}\tau, \quad (12)$$

式中：$\partial\Omega$为 Ω的边界。由此可求出

$$u(r,t)=\int_0^t\mathrm{d}\tau\int_a^b G(r,\xi,t,\tau)f(r,t)\mathrm{d}\xi+$$

$$\int_a^b G(r,\xi,t,0)T_0\mathrm{d}\xi。\quad (13)$$

2 解析近似解与参数选择

感应钎焊时工件置于感应线圈产生的交变磁场中，由此产生的感应电流将工件加热。感应电流的强度与回路中交流电的频率成正比，频率高，感应电流大，加热速度快；但频率越高，交流电的集肤效应越明显，加热的厚度越薄，工件内部只能依靠表面层向内部的导热来加热，加热不均匀程度增大。此外，电流渗透深度又与材料的电导率和磁导率有关。电导率越小，电流渗透深度越深，表面效应越小；磁导率越小，电流的渗透深度也越大。钢在室温下的磁导率较大，但在超过 768 ℃后磁导率成倍减少，而且钢的电导率又比较小，故表面效应小，钎焊时可采用较高的频率，一般使用不低于 10 kHz的高频感应电流。铜和铝的磁导率虽小，但电导率比钢大得多，电流渗透深度较小，因此频率的选择对于这类材料的钎焊工艺很重要。

图 2为不同频率下铜管道内的感应电流密度沿半径的分布曲线。管道外径为 18 mm，壁厚 1.4 mm。铜的电导率为 3.92×10^6 S/m，磁导率为 $4\pi\times10^{-7}$ H/m。频率 $f_1\sim f_5$的大小分别为300 kHz，100 kHz，50 kHz，20 kHz，7 kHz。由图可见，对于壁厚为 1.4 mm 的铜管道的感应加热，可以选用频率为 50 kHz的电流。试验中将熔点为 575 ℃的钎料环分别固定于管道内外，电流大小为 120 A，频率为 50 kHz，观察到加热 28 s后，外壁上的钎料环开始熔化，随后 2 s内，内壁上的钎料环也开始熔化。

图 3为不同频率下铝管道内的感应电流密度沿半径的分布曲线。管道外径为 16 mm，壁厚 3 mm。铝的电导率为 2×10^7 m/S，磁导率为 $4\pi\times10^{-7}$ m/H。频率 $f_1\sim f_5$的大小分别为 10 kHz，7 kHz，4 kHz，2 kHz，700 Hz。由图可见，对于壁厚为 3 mm 的铝管道的感应加热，可以选用频率为 4 kHz的电流。试

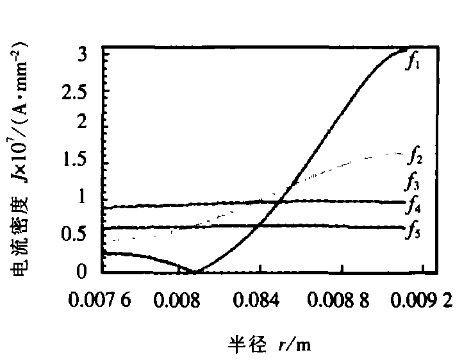

图 2 铜管道内感应电流密度分布

Fig. 2 Distribution of induction current in copper pipe

验中将熔点为 575 ℃的钎料环分别固定于管道内外，电流大小为 120A，频率为 50 kHz 观察到加热 24 s后，外壁上的钎料环开始熔化，但随后在内壁上的钎料环熔化之前，铝管道已先熔化。

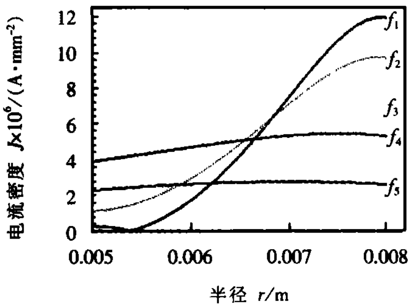

图 3　铝管道内感应电流密度分布

Fig. 3　Distribution of induction current in aluminium pipe

上述试验结果表明，对于管道的感应加热，利用式(12)和式(13)的解选择频率比传统的经验公式 $\delta=\sqrt{2/\omega\mu\sigma}$ 更精确。因为后者由平面电磁波在导电媒质中的传播特性导出，因此更适合于板状结构感应加热时频率的选择。

3　结　　论

(1) 采用计算机数值分析手段建立了感应加热电源及其频率范围的选择数值分析模型，模型表明，数值解析法可以作为高频感应钎焊感应加热设备设计的重要方法。

(2) 在对高频电源电流频率等参数的选择时，利用数值解析模型所得到的解析近似解进行频率选择比传统经验公式 $\delta=\sqrt{2/\omega\mu\sigma}$ 精确，因为后者由平面电磁波在导电媒质中的传播特性导出，更适合于板状结构感应加热时频率的选择，而对于管状或其它复杂形状，利用数值解析解可以较好的对高频电源的频率进行优化选择。

参考文献：

[1] Webb J P, Forghani B. DC current distributions and magnetic fields using the t-omega edge element methods[J]. IEEE Trans On Magnetics, 1995, 31(3): 1444－1447.

[2] Dular P, Nicolet A, Genon A, et al. A discrete sequence associated with mixed finite elements and its gauge condition for vector potentials[J]. IEEE Trans on Magnetics, 1995, 31(3): 1356－1359.

[3] 罗春荣，陆建隆．电动力学[M]．西安：西安交通大学出版社，2000.

[4] 马信山，张济世，王　平．电磁场基础[M]．北京：清华大学出版社，1995.

[5] 王纪林，向光辉．特殊函数与数学物理方程[M]．上海：上海交通大学出版社，2000. 160－176.

[6] 符果行．经典电磁理论方法[M]．北京：电子科技大学出版社，1998. 130－132.

[7] 薛兴恒．数学物理偏微分方程[M]．合肥：中国科学技术大学出版社，1995. 303－306.

[8] 冯吉才，何　鹏，刘会杰，等．高频感应钎焊中电源频率的优化选择[A]．第十二届全国钎焊及特种连接技术交流会论文集[C]．青岛，2002. 232－240.

作者简介：何　鹏，男，1972年生，工学博士，副教授。研究方向为钎焊、扩散焊，发表论文 60余篇。

Email: hepeng@hit.edu.cn

Key words: high temperature polymer matrix composite material; ceramic coating; erosion; thermal-resistance coating

Dynamic behavior of plasma in CO_2 laser welding of stainless steel

DUAN Ai-qin[1,2], CHEN Li[1,2], WANG Ya-jun[2], HU Lun-ji[1] (1. Huazhong University of Technology and Science, Wuhan 430074, China; 2. BAMTRI, Key laboratory for high energy density beam processing technology, Beijing 100024, China). p17 – 20

Abstract: Laser induced plasma is an important physical phenomenon in laser deep penetration welding. It has stronger relationsip to stability of process, quality of weld, and efficiency of laser energy. In this paper, two methods were used to study the dynamic behavior of plasma and the influences on stability of welding process. These methods were high-speed camera and optical signal monitoring. The results showed that the dynamic process of plasma can be divided into four steps, (1) material vaporing; (2) plasma increasing; (3) plasma bombing and separating; (4) plasma scattering . The main reason affected welding process stability is the fluctuation of plasma between non-penetration and penetration process.

Key words: Laser welding; laser induced-plasma; high-speed camera; optical signal

Weld residual stress distribution of GH536 superalloy with EBW measuned by Mathar method

FU Peng-fei, LIU Fang-jun, FU Gang, MAO Zhi-yong (Key Laboratory of high energy density beam processing technology, Beijing Aeronautical Manufacturing Technology Research Institute, Beijing 100024, China). p21 – 23

Abstract: Electron beam welding is applied to manufacturing many superalloy components of aeroengine, but the researches of weld residual stress were very few for those components. In this paper, weld residual stress of GH536 superalloy components with EBW were measured by Mathar method. Test results showed that residual stress is low in the weld and its distribution accords with the traditional rules. This research can accumulate experiences and properties data for manufacturing aeroengine components with EBW.

Key words: GH536 superalloy; electron beam welding; hole drilling method; residual stress

Real-time monitor system based on virtual instrument technology for laser welding

ZHANG Pu, PENG Qi-zhi, KONG Li (Huazhong University of Technology and Science, Wuhan 430074, China). p24 – 26

Abstract: The laser deep penetration welding monitoring system based on the virtual instrument technology was introduced. The component of hardware and the development of software were illuminated. Three signals of ultraviolet light, infrared light and acoustic signal acquired by three special sensors. The raw data were processed dy DSP, multi-sensors data fusion was done by neural network algorithm, and the reliable result of welding quality was oslained. The experimental data proved the system's validity and stability.

Key words: virtual instrument; laser welding; data fusion

Optimization selection of power source frequency in high frequency induction brazing

HE Peng, LIU Duo, FENG Ji-cai (National Key Laboratory of Advanced Welding Production Technology, Harbin Institute of Technology, Harbin 150001, China). p27 – 29

Abstract: Appropriate frequency of high frequency power source shoulded be selected to obtain perfect soldered joint during high frequency induction brazing according to the physical performance of joint materials. Numerical selection model for the frequency and its arrange of high frequency induction heating power source was set up by means of numerical analysis. It showed that numerical analysis can be used as an important artifice for design of high frequency power equipment. Compared the analytical results from the numerical model with that of the traditional formula, it showed that the former is more accurate. Because the latter was derived from the plane electromagnetic wave spreading characteristic in electro-conductive inter-media, it was more suitable for the frequency selection of board structure high frequency induction heating. But for frequency selection of pipe-structure or more complex structure high frequency induction heating, the numerical analytical method will be better.

Key words: high frequency induction brazing; power frequency; numerical analysis

Corrosion behavior of weld metal of low-alloy steel

HUANG An-guo[1], LI Zhi-yuan[1], YU Sheng-fu[1], ZHOU Long-zao[1], ZHANG Guo-dong[2] (1. School of Materials Science and Engineering, Huazhong University of Science and Technology, Wuhan 430074, China; 2. School of Power and Mechanic, Wuhan Uniersity, Wuhan 430072, China). p30 – 34

Abstract: Two welding heat input were applied to 16Mn and X70 steel by SAW. The corrosion behavior of weld metal was investigated in two kinds of solution, NACE and 3.5% NaCl, respectively. The results show that corrosion tendency of acicular ferrite (AF) in weld is greater than other microstructures, but its corrosion velocity is slowly. The corrosion resistance of weld metal with AF increases with the increasing of ac-